Comparison of current-voltage characteristics for hypothetic Si and SiC bipolar junction transistor

Tomislav Matić, Tomislav Švedek, Marijan Herceg

Department of Communications, Faculty of Electrical Engineering, J.J.Strossmayer University of Osijek
E-mail: tmatic@etfos.hr, svedek@etfos.hr, marijan.herceg@etfos.hr

Abstract. The paper presents a model developed for numerical simulation of temperature dependence of a hypothetical Si and SiC diode and BJT current-voltage characteristics. A classical Si PN wide-base diode model and an E-M BJT model are used with SiC semiconductor-specific parameters. Intrinsic carrier concentrations, carrier mobility temperature and doping concentration dependence are calculated for both semiconductors. The obtained current-voltage characteristics are compared and their temperature dependence is discussed. A hypothetic SiC PN diode has a much higher knee voltage and a wider extrinsic or operating temperature range, and the same applies to SiC BJT, which altogether makes SiC devices more appropriate for high-temperature and high-power applications.

Keywords: silicon carbide, PN diode, BJT transistor, temperature characteristic, Ebers-Moll model

Primerjava tokovno-napetostne karakteristike hipotetičnih Si in SiC bipolarnih transistorjev

Povzetek. Prispevek predstavlja razvoj modela za numerično simulacijo temperaturne odvisnosti hipotetične Si in SiC diode ter tokovno-napetostne karakteristike bipolarnega transistorja. Uporabljen je klasični Si PN model diode in Ebers-Mollov model transistorja s specifičnimi parametri polprevodnika SiC. Za oba polprevodnika smo izračunali intrinzične koncentracije nosilcev, temperaturno mobilnost in vpliv koncentracije dopiranja. Naredili smo primerjavo dobljenih tokovno-napetostnih karakteristik in temperaturnih odvosnosti. Hipotetična SiC PN dioda ima precej višjo kolensko napetost in širše temperaturno območje, podobno velja tudi za SiC bipolarni transistor. Takšna elementa sta primerna za uporabo pri visokih temperaturah in močeh.

Ključne besede: silicijev karbid, PN dioda, bipolarni transistor, temperaturna karatkeristika, Ebers-Mollov model

1 Introduction

Silicon carbide (SiC) is a wide energy band-gap semiconductor. It has been developed for the use in high-temperature, high-power or high-radiation conditions under which conventional semicon-ductors, such as silicon (Si), cannot function. SiC can be used as a material for high-temperature operating (650 °C) gas sensors as well as for pressure sensors and accelerometers for automotive and space industry applications using micro-electromechanical systems (MEMS) [1]. Silicon carbide comes in a variety of crystal structures called polytypes. Each SiC polytype has its own distinct set of electronic properties. Basic SiC polytypes are 3C-SiC, 4H-SiC and 6H-SiC. The only form of SiC with a cubic crystal structure is 3C-SiC, also known as β-SiC. The other two polytypes, 4H-SiC and 6H-SiC, are two of many possible SiC polytypes with a hexagonal crystal structure [2]. Prototypes of SiC bipolar junction transistors (BJT) still exhibit poor gains, but improvements in SiC crystal growth and surface passivation will greatly improve SiC BJT gain and make SiC bipolar devices a more viable technology [2]. Thereby, it seems valuable to do the comparison of current-voltage characteristics of hypothetic Si and SiC BJTs, especially concerning their operating temperature ranges.

The basic idea behind this work is shown in Figure 1., where assumption is made that models developed for Si PN diode and BJT can be used as the first-order models of SiC devices, by simply introducing SiC-specific semiconductor parameters (E_G, n_i, $\mu_{n,p}(N,T)$). With the same geometric parameters for hypothetic Si and SiC devices, resulting voltage-current characteristics for the SiC PN diode and BJT can be compared to their Si counterparts. The comparison of Si and SiC characteristics points out why the SiC is such a promising semiconductor in high-temperature, high-power and high-radiation applications.

The sets of basic equations for intrinsic carrier concentrations and carrier mobilities of Si and SiC semiconductors are described in Section II. Section III presents mathematical models of Si and SiC PN diodes, simulated voltage-current characteristics and their temperature dependence. In Section IV basic equations of the Ebers-Moll model of the Si and the SiC BJT are given, and resulting simulated input and output voltage-

current characteristics are discussed. Some concluding remarks are given in Section V.
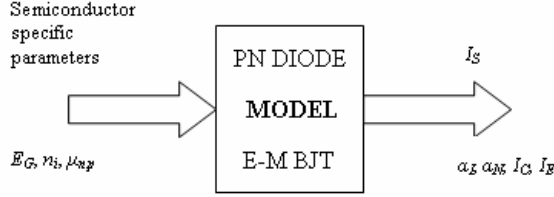

Figure 1. Basic PN diode and Ebers-Moll bipolar junction transistor model for SiC semiconductor

2 Electrical properties of Si and SiC semiconductor materials

Properties of a semiconductor material induce temperature and power limitations in semiconductor device application. Table 1 shows basic electrical properties of contemporary semiconductor materials [1], [2], [4], [5]. From the table it can be deduced that basic properties of SiC are desirable for high-power electronic-device operation.

Because of the wide energy band-gap, SiC electronic devices can operate at extremely high temperatures without suffering from intrinsic conduction effect. With higher thermal conductivity than any metal and almost seven times greater electrical breakdown field strength than Si or GaAs, SiC can operate at extremely high-power levels and dissipate a large amount of excess heat generated, and SiC electronic devices can be used in high-voltage and high-power applications [3].

Table 1. Properties of some semiconductor materials (T = 300 K)

	Si	GaAs	4H-SiC
E_G(eV)	1.1	1.4	3.26
ε_r	11.8	12.8	10
E_C(MV/cm)	0.3	0.4	2.2
v_{sat}(10^7cm/s)	1	2	2
μ_n(cm^2/Vs)	1430	8500	947
μ_p(cm^2/Vs)	460	400	140
λ(W/cmK)	1.5	0.5	5

2.1 Intrinsic carrier concentration

The fundamental electric parameter of a semicon-ductor is intrinsic carrier concentration - n_i, which also defines a high-temperature operating limit of the semiconductor device. The following equation describes temperature dependence of intrinsic carrier concentration for Si [6]:

$$n_i = CT^{\frac{3}{2}} \exp\left(-\frac{E_G(T)}{E_T}\right) \quad , \quad (1)$$

where C = $7.2 \cdot 10^{15}$ cm^{-3}/K$^{3/2}$, E_T = kT/q, k is the Boltzmann's constant, q is the electron charge and $E_G(T)$ is the energy band-gap, for Si defined as:

$$E_G(T) = 1.175 - 9.025 \cdot 10^{-5}T - 3.05 \cdot 10^{-7}T^2 \quad . (2)$$

The relationship between intrinsic carrier concentration and temperature for SiC is given in [6] as:

$$n_i = \sqrt{N_C(T)N_V(T)} \exp\left(-\frac{E_G(T)}{2E_T}\right) \quad , \quad (3)$$

where $N_C(T)$ and $N_V(T)$ are effective densities of states in conduction and valence band, respectively:

$$N_C(T) = 2\left(\frac{2m_e^* kT}{\hbar^2}\right)^{\frac{3}{2}} = \left(\frac{T}{300}\right)^{\frac{3}{2}} N_C(300) \quad , \quad (4)$$

$$N_V(T) = 2\left(\frac{2m_h^* kT}{\hbar^2}\right)^{\frac{3}{2}} = \left(\frac{T}{300}\right)^{\frac{3}{2}} N_V(300) \quad . \quad (5)$$

(In Eq. (4) and Eq. (5), m_e^* and m_h^* stand for effective mass of electron and hole, respectively, and $\hbar$ is the Planck's constant.)

Temperature dependence of the SiC band-gap is given by the following equation:

$$E_G(T) = E_G(300) + a\left(\frac{300^2}{300+b} - \frac{T^2}{T+b}\right) \quad . \quad (6)$$

Table 2. Intrinsic carrier concentration parameters for SiC (T = 300K)

	4H-SiC
N_C(300) cm^{-3}	$1.66 * 10^{19}$
N_V(300) cm^{-3}	$3.19 * 10^{19}$
E_G(300) eV	3.26
a	$5.41 * 10^{-4}$
b	0

Table 2 shows the effective density of states in SiC conduction and valence band at room temperature (300 K), the SiC energy band-gap at room temperature, as well as a and b constants for Eq.(6).

MATLAB® is used for calculation of temperature dependence of intrinsic carrier concentration. Figure 2 shows $n_i(T)$ for both Si and SiC semiconductors. As it can be seen, intrinsic carrier concentration $n_i(T)$ for SiC remains under 10^{10} cm^{-3} for temperatures over 600 K.

Lower intrinsic carrier concentration prevents SiC suffering from intrinsic conduction effect, and maintains semiconductor electrical properties (extrinsic temperature range and consequently operating temperature of the device) at much higher temperatures than conventional semiconductors such as Si or GaAs. Figure 2 proves that SiC is good technology for high-temperature devices.
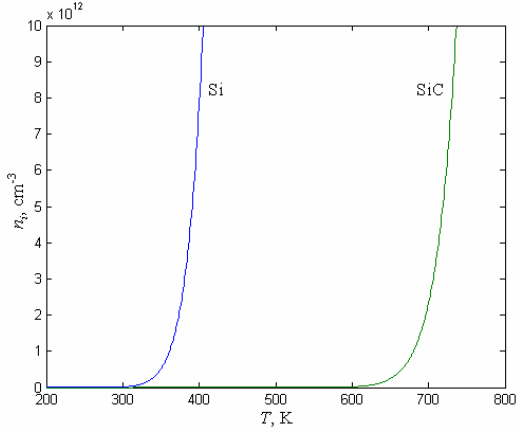
Figure 2. Intrinsic carrier concentration for Si and SiC as a function of temperature

2.2 Carrier mobility

Two basic types of scattering affect carrier mobility: lattice and impurity scattering. Calculation of carrier mobility dependence on temperature and doping concentration in Si can be carried out by the following equation [4]:

$$\mu_{n,p}(T) = \mu_{\min}(T) + \frac{\mu_{\max}(T) - \mu_{\min}(T)}{1 + \left(\dfrac{N_A + N_D}{N_{ref}(T)}\right)^{c(T)}} \quad , \quad (7)$$

where N_D and N_A are the donor and acceptor concentrations; temperature dependence of mobility constants are defined by the following equations [5]:

$$\mu_{n,\max} = \mu_{n,\max}(300) \cdot \left(\frac{300}{T}\right)^2 \quad , \quad (8)$$

$$\mu_{p,\max} = \mu_{p,\max}(300) \cdot \left(\frac{300}{T}\right)^{2.18} \quad , \quad (9)$$

$$\mu_{n,p\ \min} = \mu_{n,p\ \min}(300) \cdot \left(\frac{300}{T}\right)^{0.45} \quad , \quad (10)$$

$$N_{ref}(T) = N_{ref}(300) \cdot \left(\frac{300}{T}\right)^{-3.2} \quad , \quad (11)$$

$$c(T) = c(300) \cdot \left(\frac{300}{T}\right)^{-0.065} \quad , \quad (12)$$

and room-temperature constants for calculation of carrier mobility in silicon are given in Table 3.

Table 3. Mobility constants for Si at $T = 300$ K

	$\mu_{\min}$, cm^2/Vs	$\mu_{\max}$, cm^2/Vs	N_{ref}, cm^{-3}	c
n	80	1430	$1.12*10^{17}$	0.72
p	45	460	$2.23*10^{17}$	0.72

Table 4. Mobility constants in 4H-SiC

	μ_{min}, cm^2/Vs	μ_{max}, cm^2/Vs	N_{ref}, cm^{-3}	e	d
n	0	947	$1.94*10^{17}$	0.61	−2.15
p	15.9	124	$1.76*10^{19}$	0.34	−2.15

The Arora's model [1] is used for calculation of the effect of doping concentration and temperature on carrier mobility in SiC. The low-field mobility is given by:

$$\mu_{n,p} = \mu_{n,p,\min}\left(\frac{T}{300}\right)^{d_{n,p}} + \\ + \frac{\mu_{n,p,\max}}{1 + \left(\dfrac{N_D + N_A}{N_{n,p,ref}}\right)^{e_{n,p}}}\left(\frac{T}{300}\right)^{d_{n,p}} \quad , \quad (13)$$

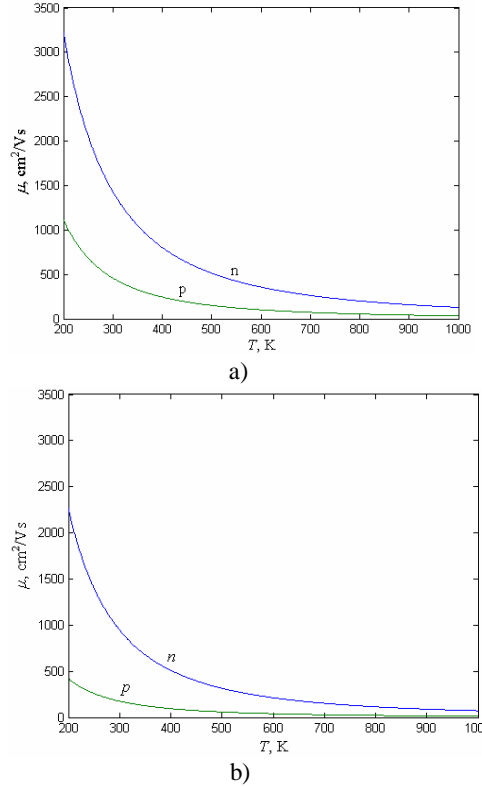where constants for calculation of carrier mobility in 4H-SiC are shown in Table 4.

a)

b)

Figure 3. Temperature dependence of mobility μ(T) for a) Si and b) SiC

Figure 3. shows electron and hole mobility for intrinsic Si (a) and SiC (b) as a function of temperature $\mu(T)$. Mobility of electrons and holes in SiC, at $T = 300$ K, is two/four times lower than the mobility of

electrons/holes in a Si semiconductor. The main reason for that is the structure of SiC, which has 50 % of carbon atoms that decrease carrier mobility.

Variation of electron and hole carrier mobility $\mu(N_D, N_A)$ with donor and acceptor doping concentrations at room temperature (300 K) is shown in Figure 4. Impurity scattering increases with higher doping concentrations whereas mobility decreases appropriately. Hole concentration in SiC is very small and its mobility is not very much impacted by the increase in doping acceptors.

2.3 I-U characteristic of hypothetic wide-base Si and SiC PN diode

A current-voltage characteristic of an ideal PN junction is described by a well-known Shockley's equation, where I_S stands for reverse saturation current in a PN junction, U is diode voltage and U_T is voltage equivalent of temperature (kT/q):

$$I = I_S\left[\exp\left(\frac{U}{U_T}\right) - 1\right] \quad , \qquad (14)$$
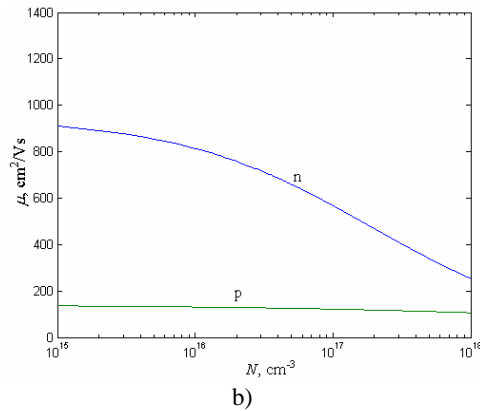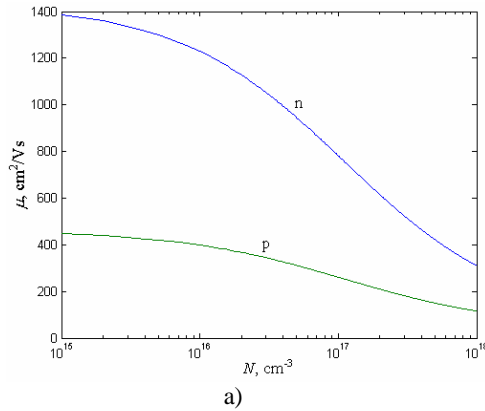

a)

b)

Figure 4. Carrier mobility dependence on doping concentrations for a) Si and b) SiC, at $T = 300$ K.

For PN diodes whose electron and hole effective diffusion lengths L_n and L_p are much shorter than W_P and W_N sides of a diode (wide-base PN diodes), reverse saturation current is equal to:

$$I_S = qS\left(\frac{n_{p0}D_n}{L_n} + \frac{p_{n0}D_p}{L_p}\right) \qquad , \qquad (15)$$

where n_{p0} and p_{n0} are equilibrium minority carrier concentrations of P and N sides, L_n and L_p are electron and hole effective diffusion lengths, D_n and D_p are electron and hole diffusion coefficients, and S is the cross-sectional area of the junction.

According to the mass action law, minority carrier concentrations can be expressed by:

$$n_{p0} = \frac{n_i^2}{p_{p0}} \quad , \qquad (16)$$

$$p_{n0} = \frac{n_i^2}{n_{n0}} \quad , \qquad (17)$$

where $p_{p0} \approx N_A$ and $n_{n0} \approx N_D$, for $N_A \gg n_i$ and $N_D \gg n_i$, and all dopands are ionized. Reverse saturation current of a diode can be now rewritten as:

$$I_S = qSn_i^2\left(\frac{D_n}{N_A L_n} + \frac{D_p}{N_D Lp}\right) \quad , \qquad (17)$$

and diffusion lengths substituted by:

$$L_{n,p} = \sqrt{D_{n,p}\tau_{n,p}} \quad , \qquad (18)$$

whereas τ_n and τ_p are electron and hole lifetimes. For diffusion coefficients calculated from Einstein relation ($D_{n,p} = \mu_{n,p}U_T$), the reverse saturation current of a diode finally becomes equal to:

$$I_S = qSn_i^2\sqrt{U_T}\left(\frac{1}{N_A}\sqrt{\frac{\mu_n}{\tau_n}} + \frac{1}{N_D}\sqrt{\frac{\mu_p}{\tau_p}}\right). \qquad (19)$$

Equation (19) is now prepared for calculation of a PN diode reverse saturation current using known SiC specific parameters ($n_i(E_G, T)$ and $\mu_{n,p}(N,T)$). Figure 5 shows MATLAB®-simulated forward-bias I-U characteristics of hypothetic Si and SiC wide-base PN diodes with equal P-side and N-side doping concentrations $N_A = N_D = 10^{16}$ cm^{-3}, electron and hole lifetimes of minority carriers presumed to be $\tau_n = \tau_p = 100$ ns, and the cross-sectional area of the junction $S = 1$ mm^2, for temperature span from 250 to 350 K. In this figure I-U characteristic of the SiC diode at 600 K is also shown. Table 5 shows reverse saturation current I_S and knee-voltage U_0 for Si and SiC, at $T = 300$ K.

Table 5. Reverse saturation current and knee-voltage for Si and SiC, at $T = 300$ K

Diode	3 I_S, A	U_0, V
Si	$9.48 \cdot 10^{-13}$	0.50
SiC	$7.92 \cdot 10^{-42}$	2.25

Comparison of forward-bias *I-U* characteristics of the hypothetic Si and SiC PN diode models at equal temperatures reveals that a SiC diode has almost five times higher knee-voltage U_0. This is the outcome of a very wide energy band-gap, and therefore, very small reverse saturation current of a SiC diode. Reverse saturation current values of a SiC diode become similar to Si diode values only at higher temperatures (around 600 K). At these temperatures the knee voltage also lowers, but the SiC diode still retains its rectifier capabilities, providing therefore a much wider extrinsic or operating temperature range of SiC devices.
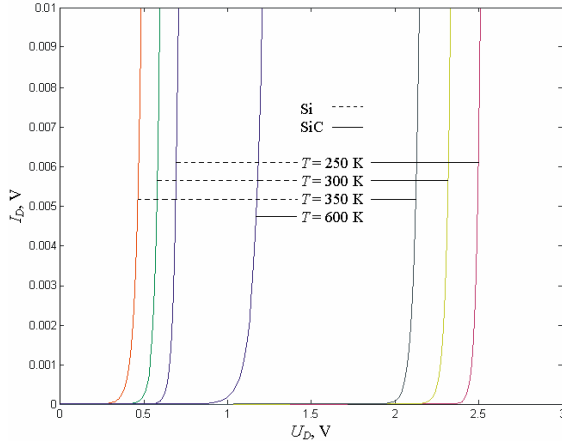

Figure 5. Forward-bias current-voltage characteristic of hypothetic Si and SiC PN diode as a function of temperature

Figure 6 displays a) reverse saturation current of Si for temperatures of 300 K and 301 K, and b) reverse saturation current of a SiC diode for the same temperatures. Temperature coefficient of the reverse saturation current is positive and approximately two times higher for a SiC than for a Si diode.

Temperature dependence of the PN diode can be described by the following equations:

$$\frac{\left(\dfrac{\Delta I_S}{\Delta T} \right)}{I_S} = \frac{3 + \dfrac{E_G}{kT}}{T} \quad , \qquad (20)$$

$$\left(\frac{\Delta I}{\Delta T} \right)_{U=const.} = \frac{I}{T} \left(3 + \frac{E_G - qU}{kT} \right) \quad , \qquad (21)$$

$$\left(\frac{\Delta U}{\Delta T} \right)_{I=const.} = \frac{U}{T} - \frac{\left(E_G + \dfrac{3kT}{q} \right)}{T} \quad , \qquad (22)$$

where Eq. (20) describes the relative temperature coefficient of reverse saturation current, Eq. (21) the temperature coefficient of forward-biased current for diode constant voltage, and Eq. (22) the temperature coefficient of forward-biased voltage for diode constant current.
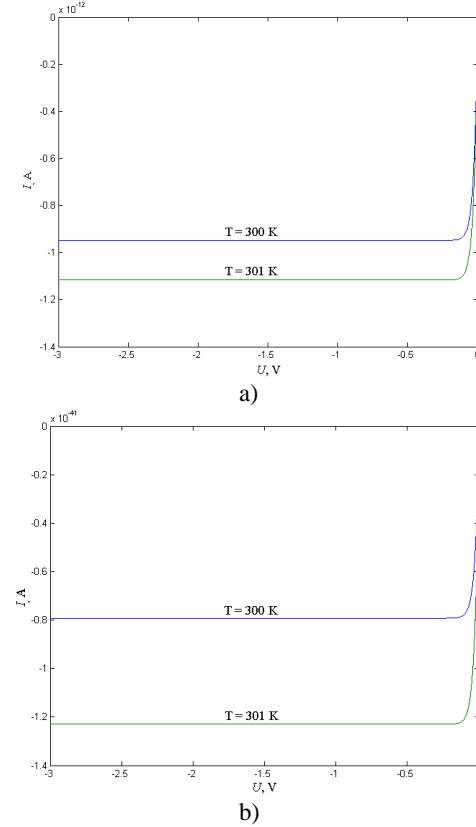

a)

b)

Figure 6. Reverse saturation current of a) Si and b) SiC diode at temperatures 300 K and 301 K, respectively

All temperature coefficients can be determined A) from Eq. (20) through (22), or B) from Shockley's equation (14). Calculation for forward-biased diodes was carried out at T = 300 K, for forward-bias diode currents of $I =$ 1 mA, and at diode voltages $U = 0.537$ V for Si and $U =$ 2.268 V for SiC. Temperature coefficient values obtained in these two ways are shown altogether in Table 6.

Table 6. Temperature coefficients of I_S, I, and U, for Si and SiC diode at $T = 300$ K, calculated by A) Eq. (20) to (22), and B) by Shockley equation (14).

Temperature	Si		SiC	
coefficients	A	B	A	B
$\left(\dfrac{\Delta I_S}{\Delta T}\right)\!\Big/ I_S$ [K^{-1}]	0.15	0.18	0.43	0.36
$\left(\dfrac{\Delta I}{\Delta T}\right)_{U=const.}$ [mAK^{-1}]	0.78	0.9	1.3	1.5
$\left(\dfrac{\Delta U}{\Delta T}\right)_{I=const.}$ [mVK^{-1}]	-2	-2.2	-3.4	-3.6

The difference in results is significant, because relations (20) through (22) are obtained by assuming that D_p, D_n, L_p, and L_n are temperature invariant, and $E_G(T)$ is linearized in the vicinity of $T = 300$ K, but they both clearly show that the temperature change of SiC characteristics is faster than that for a Si diode.

4 Ebers-Moll model of bipolar junction transistor

In the Ebers-Moll model of an NPN bipolar junction transistor (BJT) linear excess electron distribution in the base can be separated into components of normal and inverse direction. Total emitter and collector currents are combinations of emitter and collector currents for both normal and inverse directions (I_{EN}, I_{CN}, I_{EI}, I_{CI}). Injection current components I_{EN} and I_{CI} are defined by Shockley equation for emitter-base and collector-base PN junctions:

$$I_{EN} = I_{ES}\left[\exp\left(-\frac{U_{EB}}{U_T}\right) - 1\right] \qquad , \qquad (23)$$

$$I_{CI} = I_{CS}\left[\exp\left(-\frac{U_{CB}}{U_T}\right) - 1\right] \qquad , \qquad (24)$$

where I_{ES} is a reverse current of the emitter-base junction for a shortened collector-base junction and I_{CS} is a reverse current of the collector-base junction for a shortened emitter-base junction. Current collection components are defined as:

$$I_{EI} = \alpha_I I_{CI} = \alpha_I I_{CS}\left[\exp\left(-\frac{U_{CB}}{U_T}\right) - 1\right] \quad , \quad (25)$$

$$I_{CN} = \alpha_N I_{EN} = \alpha_N I_{ES}\left[\exp\left(-\frac{U_{EB}}{U_T}\right) - 1\right] \quad , \quad (26)$$

where α_N and α_I are normal and inverse active-mode current gain factors of NPN BJT in common-base (CB) configuration.

Total emitter and collector currents are superposition of all four current components:

$$I_E = I_{ES}\left[\exp\left(-\frac{U_{EB}}{U_T}\right) - 1\right] - \alpha_I I_{CS}\left[\exp\left(-\frac{U_{CB}}{U_T}\right) - 1\right] \quad (27)$$

$$I_C = \alpha_N I_{ES}\left[\exp\left(-\frac{U_{EB}}{U_T}\right) - 1\right] - I_{CS}\left[\exp\left(-\frac{U_{CB}}{U_T}\right) - 1\right] (28)$$

By Eq. (27) and (28) it is possible to derive input and output *I-U* characteristics of a bipolar junction transistor. For CB configuration of NPN BJT, input characteristics are defined as $I_E = \mathrm{f}(U_{EB}, U_{CB})$:

$$I_E = I_{ES}\left[\exp\left(-\frac{U_{EB}}{U_T}\right) - 1\right] - \alpha_N I_{ES}\left[\exp\left(-\frac{U_{CB}}{U_T}\right) - 1\right]$$
$$(29)$$

and output characteristics as $I_C = \mathrm{f}(U_{CB}, I_E)$:

$$I_C = \alpha_N I_E - I_{CB0}\left[\exp\left(-\frac{U_{CB}}{U_T}\right) - 1\right] \quad , \qquad (30)$$

where:

$$I_{CB0} = (1 - \alpha_I \alpha_N) I_{CS} \quad , \qquad (31)$$

and I_{CB0} is reverse saturation current of a collector-base PN junction for the opened emitter-base PN junction.

Normal and inverse active-mode current gain factors of NPN BJT in common-base configuration, α_I and α_N, depend on geometry and technology of the transistor as well as on Early effect. If we take the aforementioned into account, they can be expressed as:

$$\alpha = \beta^* \gamma \quad , \qquad (32)$$

where β^* is the base transport factor, and γ is the emitter injection efficiency. Their geometry and technology dependence can be approximated by:

$$\beta^* = 1 - \frac{1}{2}\left(\frac{W_{Bef}}{L_{nB}}\right)^2 \qquad , \qquad (33)$$

$$\gamma = \frac{1}{1 + \dfrac{\sigma_B W_{Bef}}{\sigma_E L_{pE}}} \qquad , \qquad (34)$$

where, W_{Bef} is the effective base-width defined in Eq. (35), L_{nB} and L_{pE} are diffusion length of electrons in the base and holes in the emitter, respectively, and σ_B and σ_E are specific conductivity of the base and the emitter. Assuming abrupt PN junctions, W_{Bef} can be defined as follows:

$$W_{Bef} = W_B - \sqrt{\frac{2\varepsilon(U_K - U_{CB})}{q}\left(\frac{1}{N_A} + \frac{1}{N_D}\right)}, \quad (35)$$

where W_B is a technological base-width and U_K is a contact potential of the base-collector junction.

Calculations are carried out by MATLAB® for a hypothetic Si and SiC NPN bipolar junction transistor with doping concentrations $N_{DE} = 10^{20}$ cm^{-3}, $N_{AB} = 10^{17}$ cm^{-3}, $N_{DC} = 10^{16}$ cm^{-3}, base-width $W_B = 5$ µm, carrier lifetimes in the emitter, the base and the collector equal to 100 ns, and equal cross-sectional areas of emitter-base and base-collector junctions ($S_E = S_C = 1$ mm^2).

Input current-voltage characteristics shown in Figure 7 are derived from the Ebers-Moll model for Si and SiC NPN BJT in common-base configuration and calculated for two different temperatures (300 and 350 K). They show consequently that a knee voltage for a SiC device is higher than the one for Si (see also Figure 2. for Si and SiC diodes) and that both voltages decrease with a temperature increase.
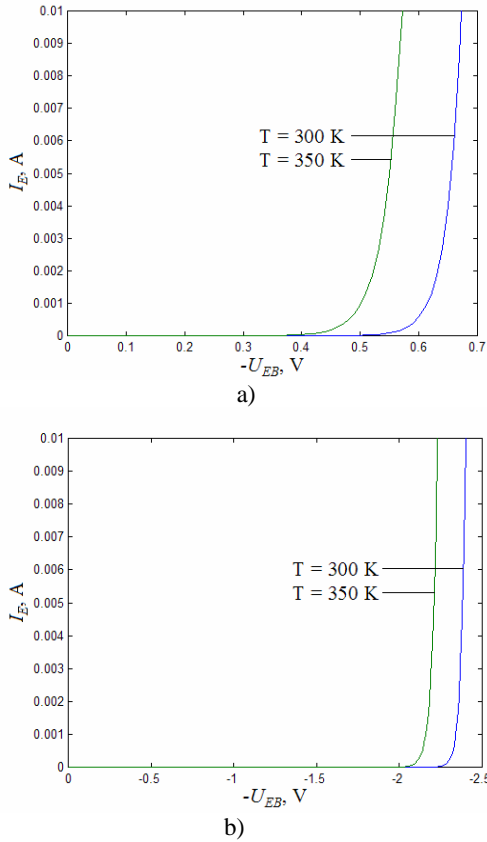
Figure 8 shows output CB current-voltage characteristics of hypothetic Si and SiC BJT which appear as a series of reverse saturation current curves of a collector-base diode, displaced by increments proportional to the emitter current. The characteristics are not flat in a normal active region, which is a consequence of the Early effect. Voltages U_{CB0} at which collector currents become zero are more negative in SiC than in Si, and absolute values of these voltages are almost equal to knee voltages of input characteristics (Table 7). With temperature increase U_{CB0} voltages became more positive, so CB output current-voltage characteristics for higher temperatures shift to the right. Current gain α for common-base configuration of a Si bipolar junction transistor is higher than the one for a SiC transistor, which can be seen in Figure 8. The reason for a higher α in a Si transistor is an almost four times higher $\sigma_E L_{pE}$ product for Si than for SiC, which affects the emitter injection efficiency γ in Eq. (32).

a)

b)

Figure 7. Input CB current-voltage characteristics of hypothetic a) Si and b) SiC NPN BJT
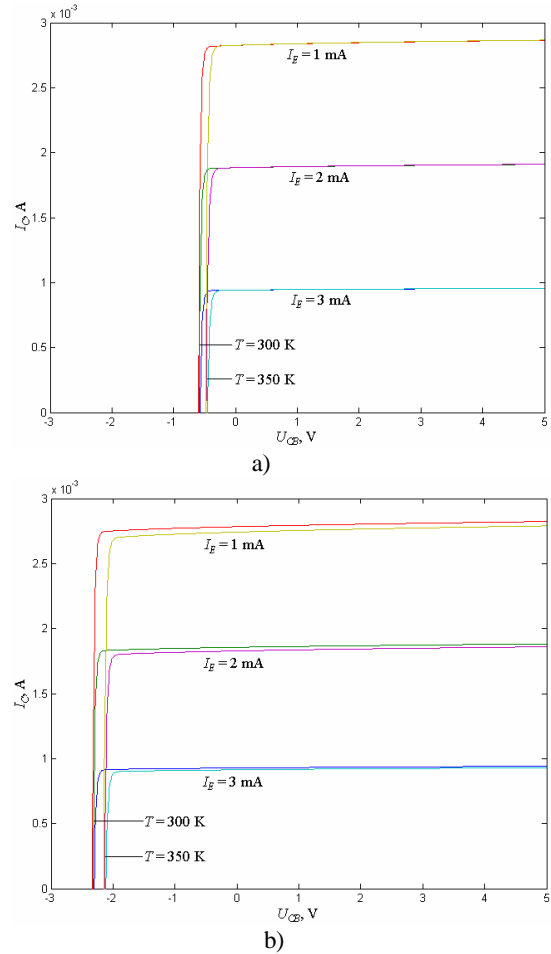

a)

b)

Figure 8. Output CB current-voltage characteristic for a) Si and b) SiC

Table 7. Voltages $U_{CB}(I_C = 0)$, contact potentials U_K, normal and inverse active-mode CB-current gains α_N and α_I for Si and SiC diode at $T = 300$ K

BJT	$U_{CB}(I_C = 0)$, V	U_K, V	α_I	α_N
Si	−0.65	0.75	0.4814	0.9550
SiC	−2.40	2.48	0.4694	0.9411

5 Conclusion

Physical properties such as high electric-field strength, high saturation-drift velocity and high thermal conductivity place SiC in the center of the latest semiconductor materials and devices research. Better thermal conductivity means reduction of SiC power-device heat-sink size, leading to significant reduction of the total size of the equipment (for example rectifiers, converters).

Comparing simulation results for Si and SiC, it is obvious that SiC is a more appropriate semiconductor material for realization of high-temperature and high-power devices. Wide energy band-gap and low intrinsic carrier concentration in SiC provides a much wider extrinsic or operating temperature range than in Si. Robust circuit designs that accommodate large changes in device operating parameters with temperature will be necessary for circuits to function successfully over the very wide temperature ranges enabled by SiC.

6 References:

[1]   Sang-Kwon Lee, Processing and Characterization of Silicon Carbide (6H- and 4H-SiC) Contacts for High-Power and High-Temperature Device Applications, Ph.D Dissertation, KHT, Stockholm 2002.

[2]   Neudeck, P.G. SiC Technology
      The VLSI Handbook. CRC Press LLC, 2000.

[3]   M.M.Hernando, A.Fernandez, J.Garcia, D.G.Lamar, M.Rascon, Comparing Si and SiC Diode Performance in Commercial AC-to-DC Rectifiers with Power-Factor Correction, IEEE Transactions on Industrial Electronics, Vol. 53, No. 2, pp. 705-707, April 2006.

[4]   D.M.Caughey, R.E. Thomas, Carrier Mobilities in Silicon Empirically Related to Doping and Field, Proceedings IEEE, Vol. 55, pp. 2192-2193, December 1967.

[5]   A.K.Henning, N.N. Chan, J.T.Watt, J.D.Plummer, Substrate Current at Cryogenic Temperatures: Measurements and a Two-Dimensional Model for CMOS Technology, IEEE Trans. Electron Devices, vol. ED-34, pp. 64-74, January 1987.

[6]   S.M.Sze, Semiconductor Devices: Physics and Technology, John Wiley & Sons. Inc., 1985.

Tomislav Matic was born in Osijek, Croatia, on October 24, 1978. He received B.S. degree from Faculty of Electrical Engineering in Osijek on 2002. Currently he is assistant at Department of Communications at Faculty of Electrical Engineering in Osijek, where he is working towards PhD degree in Communications. He's current research interests are A/D conversion, sigma-delta A/D converters and FPGA programming for communications applications.

Tomislav Švedek received BSc, MSc and PhD degrees form Faculty of Electrical Engineering Zagreb, University of Zagreb, Croatia. He joined Institute for Electronics, Telecommunications and Automation (IETA) RIZ Zagreb, in 1975 as development engineer, PTT Project bureau, Zagreb in 1980 as project leader, Electrotechnical Institute of Rade Končar, Department for design of Integrated Circuits in 1986 as ASIC supervisor, and Faculty of Electrical Engineering, University of Osijek in 1993, as Full professor for Electronic circuits and Microelectronics. His scientific interests are design and testability of ASICs, microelectronic RF circuits, and digital modulation methods.

Marijan Herceg was born in Osijek, Croatia, in 1978. He received the B.S. degree in electrical engineering from Faculty of Electrical Engineering in Osijek, Croatia in 2002. He is currently working towards Ph.D. degree in communication and informatics at the Faculty of Electrical Engineering in Osijek, Croatia. He's research interests are advanced modulation techniques like power efficient modulations for ultra-wide band (UWB) and FPGA programming for communications applications.